EPJ Photovoltaics **6**, 60501 (2015)
www.epj-pv.org
DOI: 10.1051/epjpv/2015001

Highly transparent front electrodes with metal fingers for p-i-n thin-film silicon solar cells

Etienne Moulin[1,2,a,b,c], Thomas Christian Mathias Müller[2,c], Marek Warzecha[2,c], Andre Hoffmann[2], Ulrich Wilhelm Paetzold[2], and Urs Aeberhard[2,c]

[1] Ecole Polytechnique Fédérale de Lausanne (EPFL), Institute of Microengineering (IMT), Photovoltaics and Thin-Film Electronics Laboratory, Rue de la Maladière 71b, 2000 Neuchâtel, Switzerland
[2] IEK5-Photovoltaik, Forschungszentrum Jülich GmbH, 52425 Jülich, Germany

Received: 23 October 2014 / Received in final form: 12 January 2015 / Accepted: 15 January 2015
Published online: 9 March 2015

Abstract The optical and electrical properties of transparent conductive oxides (TCOs), traditionally used in thin-film silicon (TF-Si) solar cells as front-electrode materials, are interlinked, such that an increase in TCO transparency is generally achieved at the cost of reduced lateral conductance. Combining a highly transparent TCO front electrode of moderate conductance with metal fingers to support charge collection is a well-established technique in wafer-based technologies or for TF-Si solar cells in the substrate (n-i-p) configuration. Here, we extend this concept to TF-Si solar cells in the superstrate (p-i-n) configuration. The metal fingers are used in conjunction with a millimeter-scale textured foil, attached to the glass superstrate, which provides an antireflective and retroreflective effect; the latter effect mitigates the shadowing losses induced by the metal fingers. As a result, a substantial increase in power conversion efficiency, from 8.7% to 9.1%, is achieved for 1-μm-thick microcrystalline silicon solar cells deposited on a highly transparent thermally treated aluminum-doped zinc oxide layer combined with silver fingers, compared to cells deposited on a state-of-the-art zinc oxide layer.

1 Introduction

Optimized transparent conductive oxide (TCO) layers applied as front electrodes in thin-film silicon (TF-Si) solar cells should address two trade-offs in order to enable cells to perform well both optically and electrically. The first trade-off is related to the surface morphology of the TCO layers. To efficiently absorb light in the optically thin silicon (Si) layers, and consequently achieve high photocurrent values, an advanced light-trapping concept has to be implemented. Light trapping in TF-Si solar cells is conventionally realized by applying randomly textured TCO electrodes to scatter light and thereby elongate the light path within the absorber layers [1–6]; the compromise here resides in the fact that the TCO surface morphologies providing the most suitable light trapping in TF-Si solar cells often trigger the formation of defective porous regions in the subsequently grown Si layers, and these porous regions are detrimental for the electrical performance of the cells [7,8].

The second trade-off is related to the intrinsic properties of the applied TCO layers. TCOs should exhibit a high conductivity and a high transparency in the full spectral range of relevance for solar cells, i.e. between 300 nm and 1100 nm. As the optical and electrical properties of TCOs are interlinked via the charge-carrier density and mobility, a high transparency in the near infrared (NIR) range is generally associated with a high sheet resistance R_{sq} and vice versa [9,10]. To compare the suitability of different TCOs to be used as electrode materials, a commonly accepted figure of merit (FOM) is defined as $FOM = \sigma/\alpha$, where σ is the film conductivity in S cm^{-1} and α is its absorption coefficient in cm^{-1} at a given wavelength [11], the best TCO being the one with the highest conductivity and the lowest light absorption.

The most common TCOs used as front electrodes for TF-Si solar cells in the superstrate (p-i-n) configuration are aluminum-doped zinc oxide (ZnO:Al) deposited by sputtering [12,13], boron-doped zinc oxide (ZnO:B) grown by low-pressure chemical vapor deposition (LPCVD) [14] and fluorine-doped tin oxide (SnO_2:F) grown by atmospheric-pressure chemical vapor deposition (APCVD) [15,16].

Novel materials such as gallium-doped ZnO have been suggested as alternative compounds for use as front TCOs

[a] e-mail: etienneantoine.moulin@epfl.ch
[b] All the results presented in this work were obtained in IEK5 (Jülich). The author recently moved to EPFL (Neuchâtel).
[c] These authors contributed equally to this work.

in p-i-n solar cells [17]. Sputtered tin-doped indium oxide In_2O_3:SnO_2 (ITO) combined with a textured superstrate has also been proposed to fulfill this function [18], and more recently hydrogenated indium oxide In_2O_3:H (IOH) [19, 20]. Other approaches have also been introduced to improve the FOM of ZnO:Al front electrodes and, with it, cell performance: for instance, two-step post-deposition annealing treatments, comprising a thermal treatment under a protective layer, result in a decrease in sub-bandgap and free-carrier absorption combined with a remarkable gain in carrier mobility [9, 21, 22].

In wafer-based photovoltaic technologies or for TF-Si solar cells in the substrate (n-i-p) configuration, a metal grid is conventionally combined with the front TCO electrode to aid in lateral conduction [23, 24]; in this case, the front TCO layer usually exhibits relatively high R_{sq} (up to 100 Ω/sq) as its thickness is generally kept thin (around 70 nm) to fulfill the role of antireflective coating [25]. In the present study, we propose to extend this well-established concept to TF-Si solar cells in the superstrate (p-i-n) configuration to relax the constraint on conductance imposed on front TCOs. In particular, this approach was adopted in the framework of the "Nanospec" project, where TCOs with high transparency in the infrared spectral range (and thus moderate conductance) were required to take full advantage of up-converter systems placed behind the cell [26, 27].

Here, we show that single-junction microcrystalline silicon (μc-Si:H) solar cells with excellent electrical properties can be obtained on highly transparent TCO layers of relatively high R_{sq} (up to approximately 30 Ω/sq) fitted with silver (Ag) fingers with optimized density. We demonstrate that this optimum can be well predicted with the optoelectronic device simulator "Advanced Semiconductor Analysis" (ASA). Then, we show that the shadowing losses induced by the Ag fingers can be noticeably reduced by a transparent retroreflective textured foil placed at the air/glass interface. We highlight the relevance of the introduced concept by comparing the cell performance with that of a cell with a state-of-the-art ZnO:Al front electrode.

2 Experimental details

The p-i-n μc-Si:H solar cells were deposited on 1.1-mm-thick glass (Corning Inc.). Figure 1a illustrates the schematic cross section of a cell with Ag fingers. The Ag fingers were evaporated on glass through a stainless steel mask, which was patterned by laser scribing, providing Ag fingers with a width of approximately 100 μm or 200 μm and a thickness of around 700 nm. In this study, the height of the fingers was not varied. However, we believe that in practice, for the finger widths considered here (∼100 μm), the thickness of the fingers could certainly be further reduced, while still providing sufficient conductivity and current-collection ability. The mask was engineered in a way that various finger geometries, i.e. with varying distances between the fingers (see Fig. 1b), could be obtained simultaneously on the same glass substrate. As a front

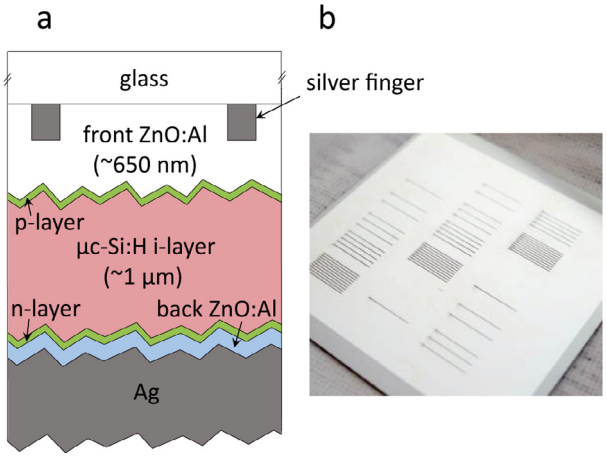

Fig. 1. (a) Schematic cross section of a μc-Si:H p-i-n solar cell deposited on a highly transparent front TCO layer with Ag fingers. (b) Evaporation mask employed to deposit the Ag fingers on the glass superstrate. The line width is varied between 100 μm and 200 μm.

electrode, a ZnO:Al bi-layer with a 1 wt.% aluminum doping concentration was deposited by radio-frequency magnetron sputtering, the first nanometers of ZnO:Al being deposited at room temperature to limit thermal stress in the Ag fingers, and the bulk ZnO:Al layer being deposited at a substrate temperature of around 300 °C. Note that, for cells with and without Ag fingers, the same front TCO was used (by co-deposition). Etching in a 0.5% w/w diluted hydrochloric acid (HCl) solution was carried out to texturize the initially smooth ZnO:Al surface, leading to a final average thickness of approximately 650 nm. The sheet resistance of the resulting ZnO:Al layers is typically around 8 Ω/sq.

In this study, a thermal treatment in vacuum (at 600 °C for 3.5 h to 5.5 h) was performed to increase the transparency of the front ZnO:Al layers fitted with the Ag fingers. A similar treatment at 400 °C did not show any noticeable modification of the opto-electrical properties of ZnO:Al. Annealing at 600 °C is challenging for industrial applications due to the severe cost issues associated to the use of Corning glass and to the thermal treatment itself. In principle, alternative TCO materials to ZnO:Al – with a higher transparency – could have been used in this study. However, one of the advantages of annealing is that it preserves the surface morphology of the front ZnO:Al [28]. It thus enables one to investigate the impact of the ZnO:Al intrinsic optical and electrical properties without considering eventual modifications of the light-trapping properties or of the Si growth conditions associated with a variation of the surface texture.

The Si layers were deposited by plasma-enhanced chemical vapor deposition (PECVD). The boron- and phosphorous-doped (p- and n-) layers and the intrinsic (i-) layer have thicknesses of approximately 20 nm and 1 μm, respectively. More details on the preparation of our baseline solar cells can be found elsewhere [29]. An 80-nm-thick sputtered ZnO:Al layer and a 700-nm-thick evaporated Ag

layer were used together as a back electrode. The cell area (of 1 cm^2) is defined by the Ag back reflector, which serves as an etching mask for the underlying ZnO:Al layer.

An antireflective/retroreflective foil from the company DSM was applied to the front side of the device at the air/glass interface. Details on the specifications and working principle of this foil are given later in the text.

The reflectance R and transmittance T of TCOs – from which their absorptance was determined (as $A = 1-R-T$) – were acquired using a LAMBDA 950 (Perkin Elmer) spectrophotometer equipped with an integrating sphere. Current-voltage (J-V) measurements were carried out using a dual-lamp solar simulator (Wacom) under standard test conditions (AM1.5G spectrum, 1000 W/m^2, 25 °C).

Simulations with ASA and model calibration

To support the measurements, full one-dimensional numerical device simulations were performed. For this purpose, we used the commercial optoelectronic device simulation software ASA [30]. The simulations account for two important aspects, namely the shadowing by the fingers and the resistive losses in the front electrode. The optical response of the solar cells was calibrated with absorptance measurements of a flat bifacial μc-Si:H p-i-n device, similar to the devices used here but without the back reflector [26]. Owing to the low coverage of the fingers (well below 5%), the additional light scattering presumably resulting from the surface modulation around the fingers has likely only a minor impact on the overall optical performance (and thus on J_{sc}). Also, due to the low height-to-width aspect ratio (<0.01) of the fingers, additional shadowing caused by illumination under oblique incidence is most probably negligible. Therefore, we assume that the 1-D model used here to account for the optical impact of the fingers already provides good estimation. The electrical parameters were derived from J-V characteristics of the device in the dark and under AM1.5G illumination. The illuminated J-V characteristics are therefore a superposition of J-V characteristics from areas in the dark (those under the fingers, J_d) and areas that receive illumination (everywhere else, J_i). The current is hence calculated as:

$$J = \frac{d_{Ag}}{d} J_d + \frac{d_{Ag-Ag}}{d} J_i,$$

where d_{Ag} is the width of a finger, d_{Ag-Ag} the gap between two adjacent fingers, and $1/d$ the finger density. Note that $d = d_{Ag-Ag} + d_{Ag}$.

Solving the differential equation for the electrostatic potential between two fingers in one dimension yields the contact series resistance

$$R_s = R_{s0} + \frac{R_{sq}^{ZnO} d_{Ag-Ag}^2}{8},$$

where R_{s0} is a constant offset (used here as a fitting parameter and set to a value of 0.08 Ω), and R_{sq}^{ZnO} the sheet resistance of the ZnO:Al front contact [26]. The variation of $1/d$ then yields – through R_s – the corresponding change in fill factor (FF), short-circuit current density (J_{sc}) and efficiency of the solar cell.

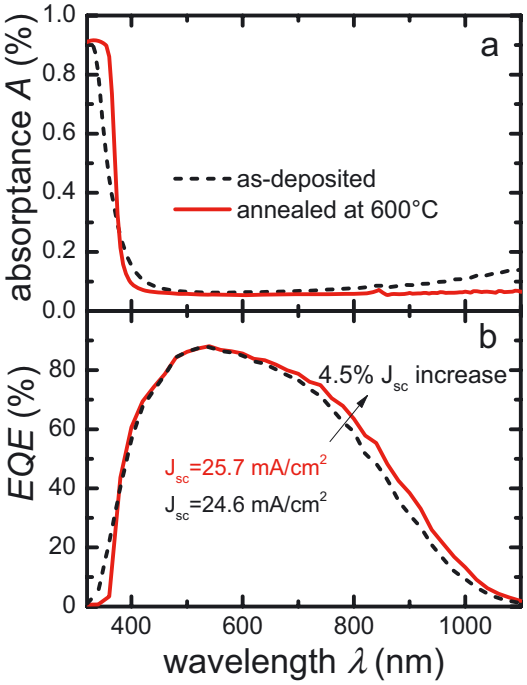

Fig. 2. (a) Absorptance A as a function of wavelength of glass/ZnO:Al superstrates with and without a post-deposition annealing treatment at 600 °C for 5.5 h. (b) External quantum efficiency EQE of the solar cells deposited on these superstrates. The corresponding photocurrent values (J_{sc}) are given in the graph.

3 Results and discussion

Figure 2 illustrates the impact of an annealing treatment on the optical properties of ZnO:Al and on the spectral performance of a complete solar cell. Below 380 nm, the ZnO:Al layer shows a higher absorptance (lower transparency) after annealing at 600 °C for 5.5 h (Fig. 2a). This effect is explained by the reduced band filling – and associated narrowing of the optical bandgap (Burstein-Moss effect) – caused by the decrease in free-carrier density upon thermal treatment [31, 32]. Above 700 nm, the reduction of the free-carrier density leads to a noticeable increase in layer transparency, which is mostly dictated by the shift of the free-electron plasma resonance towards longer wavelengths [33, 34]. Finally, sub-bandgap absorption in the spectral range below the fundamental absorption edge, i.e. from 380 nm to 500 nm, also decreases, as already reported in reference [9]. In accordance with the absorptance data of the glass/ZnO:Al superstrates, the external quantum efficiency (EQE) of the cell deposited on the annealed superstrate surpasses that of the reference cell in the near-infrared (NIR) wavelength region; this EQE gain compensates for the slight optical loss below 380 nm, such that the photocurrent increases from 24.6 mA/cm^2 to 25.7 mA/cm^2 (by 4.5%). The lower absorptance of the

treated ZnO:Al between 380 nm and 500 nm does not translate into an *EQE* gain; the optical behaviour of single layers on glass strongly differs from that of more complex optical systems like complete solar cells and further investigation would be needed to understand this effect.

Annealing ZnO:Al in vacuum at 600 °C typically results in an increase in sheet resistance, due to the decreased carrier concentration and to a lower Hall mobility [10,33]. In the literature, the latter effect is attributed to residual oxygen gas in the vacuum chamber, leading to oxygen adsorption – and thus probably to an increased barrier height – at the grain boundaries of ZnO:Al [35,36].

After 3 h of annealing at 600 °C in vacuum, the ZnO:Al layer becomes highly transparent, even though R_{sq} remains below 25 Ω/sq. Figure 3 shows the *FF*, J_{sc} and efficiency of 1-cm^2 full-area μc-Si:H cells deposited on thermally treated front ZnO:Al layers (with a R_{sq} of around 20 Ω/sq) equipped with 200-μm-wide Ag fingers. The finger density is varied from 0 (i.e. with no finger) to 10 fingers per cm. The V_{oc} exhibits almost no variation upon modification of the finger density (not shown here). Owing to the relatively thick ZnO:Al layer (of approximately 650 nm), the abruptness of the transition step at the finger edges might be strongly attenuated, preventing the occurrence of too severe structural defects in the subsequent layers that would deteriorate cell performance. The *FF* first rapidly increases from 61% to 72% by adding a single finger (see Fig. 3a, solid black line) and then saturates at a value of 74% for higher finger densities. Note that the strong benefit observed when adding a single finger is explained by the rather long distance (of around 3 mm) separating the cell edges and the bus bar where the contact is made. As expected, the J_{sc} decreases linearly with increasing Ag finger density (Fig. 3b) due to increased shadowing. The highest $FF \times J_{sc}$ product, and consequently the highest efficiency, is obtained with two fingers per cm (Fig. 3c, solid black line). The existence of this optimal configuration is in good agreement with theoretical predictions obtained with ASA (Fig. 3, dashed lines).

To improve light coupling into solar cells, an antireflective coating is traditionally applied at the air/glass interface. Geometric textures with feature sizes well above the wavelength of the incoming light can be introduced at this interface to fulfill this function [37,38]. The antireflective effect is based on the rebound of the incident light at the facets of the texture, as illustrated in Figure 4 (effect 1) for pyramidal features. One particularity of such textures is that they also permit some of the light reflected at the first interfaces (glass/ZnO:Al, ZnO:Al/Si) or at the Ag fingers to be redirected towards the absorber layer (see Fig. 4, effect 2). In the present study, the antireflective/retroreflective (AR-RR) texture is of particular importance since it mitigates the optical (shadowing) losses induced by the fingers by effectively retroreflecting the light back into the solar cell. Here, the textured cover consists of an adhesive flexible polymeric foil, from the company DSM, with a refractive index similar to that of glass, attached directly to the glass superstrate. The positive impact of the AR-RR foil on the device performance is demonstrated in Figure 3 (lines with triangles): the AR-RR foil leads to a substantial gain in J_{sc} (Fig. 3b). Note that the relative gain in J_{sc} obtained with the foil increases with finger density, which underlines the effectiveness of its retroreflective ability. As a result of this effect, a new optimum of the finger geometry is found with the AR-RR foil, which gives a maximum power conversion efficiency of approximately 9% with three fingers (per cm).

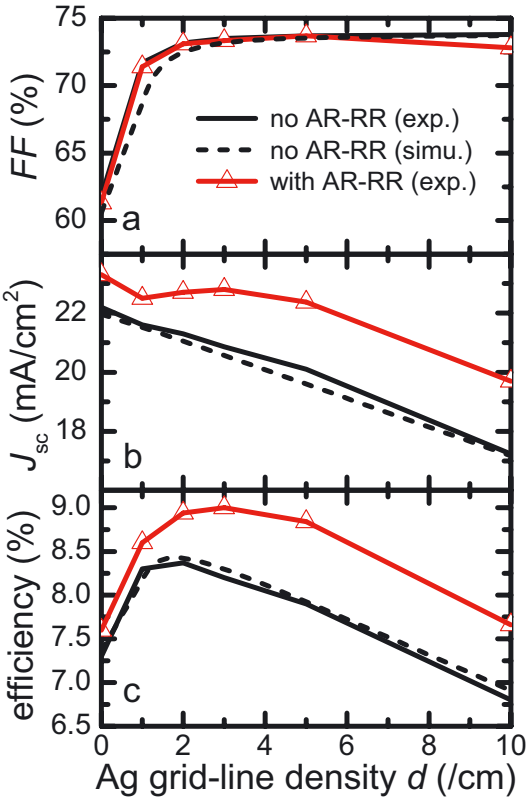

Fig. 3. Experimental and calculated parameters of μc-Si:H solar cells deposited on thermally treated front ZnO:Al layers fitted with Ag fingers of varying density. The curves with triangles represent parameters of cells with an antireflective/retroreflective (AR-RR) foil. Note that finger densities d of $0 < d < 1$ make sense only for the simulated data since the experimental parameters extracted here were measured on cells with an active area of 1×1 cm^2. The case $d = 0$ represents the cell with no Ag fingers.

By reducing the width of the fingers to 100 μm (i.e. by 50%) and by choosing a density of three fingers per cm, we were able to further increase the cell performance. Figure 5 depicts the *J-V* characteristics of a cell deposited on such a front electrode and of a reference cell, co-deposited on a bare, untreated ZnO:Al layer. The corresponding cell parameters with and without the AR-RR foil are listed in Table 1.

The major difference resides in the *FF*: The annealed ZnO:Al layer fitted with Ag fingers provides a higher *FF*, by around 2.5% (rel.), than the reference ZnO:Al electrode. This gain underlines the beneficial role of the metal fingers, which more than compensate for the increased

Table 1. *J-V* parameters of cells (average of the three best), with and without an AR-RR foil, deposited on a reference ZnO:Al layer (ref.) and on a ZnO:Al layer annealed at 600 °C for 3.5 h (ann.) fitted with Ag fingers.

	Efficiency (%)	*FF* (%)	J_{sc} (mA/cm^2)	V_{oc} (mV)
ref.	8.5	70.3	23.1	525
ref. + AR-RR	8.7	70.1	23.7	525
ann. + fingers	8.7	71.9	22.9	530
ann. + fingers + AR-RR	9.1	71.9	23.8	530

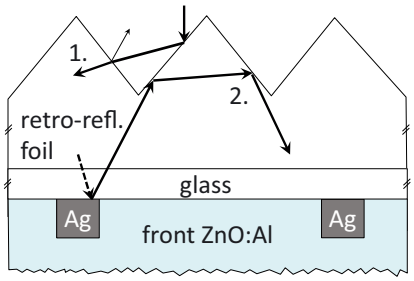

Fig. 4. Illustration of the geometric-optics interaction between a ray of light and the anti-reflective/retroreflective foil. Effect 1: the fraction of incoming light that is not transmitted into the foil upon the first incidence will hit a second facet, resulting in a higher fraction of transmitted light. Effect 2: light reflected out of the cell, in particular at the Ag fingers, is redirected back towards the active layers of the cell via a double rebound of the light beam at the textured-foil/air interface.

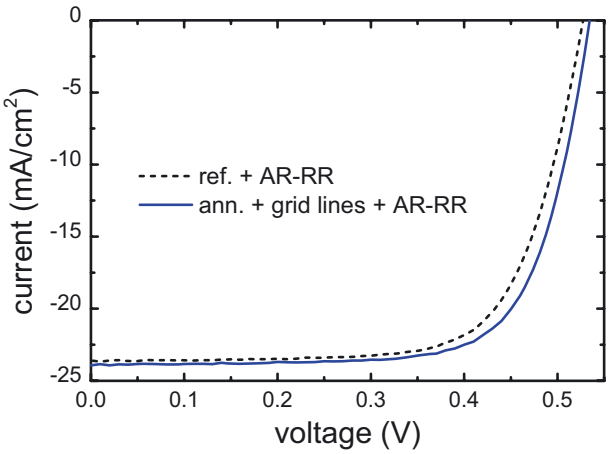

Fig. 5. *J-V* curves of 1-μm-thick μc-Si:H solar cells deposited on a reference ZnO:Al layer and on a ZnO:Al layer annealed at 600 °C for 3.5 h equipped with Ag fingers. The width of the fingers is approximately 100 μm and the density is 3 fingers per cm. Both cells are covered with an AR-RR foil.

Ohmic losses in the annealed ZnO:Al layer. For cells without an AR-RR foil, a slightly smaller J_{sc} is measured for the front electrode with Ag fingers, due to shadowing. The application of the AR-RR foil leads to a J_{sc} increase of around 2.6% for the reference cell and 4% for the cell with fingers. Notably, a slightly higher V_{oc} is measured for the cell with the annealed ZnO:Al layer (accounting for a relative efficiency gain of less than 1%). Overall, cells with the AR-RR foil are significantly improved by substituting the reference ZnO:Al layer with a highly transparent front electrode fitted with Ag fingers: The efficiency increases from 8.7% to 9.1%.

To conclude, we demonstrated that the combination of a highly transparent front TCO with metal fingers is a promising approach to obtain a better compromise between the optical and electrical constraints of TF-Si solar cell front electrodes. We highlighted the utility of this concept for 1-μm-thick μc-Si:H solar cells deposited on thermally treated ZnO:Al layers with Ag fingers, where a noticeable gain in *FF* has been measured as compared to reference cells deposited on bare, untreated ZnO:Al. By introducing a millimeter-scale textured foil providing an antireflective and retroreflective effect at the air/glass interface, we have been able to offset the impact of the shadowing losses induced by the fingers. By extending this approach to other TCO materials such as sputtered ZnO:Al with a lower doping concentration or to IOH or LPCVD-ZnO and by using optimized geometries for the metal fingers, we anticipate further advances in the efficiency of TF-Si solar cells in the single- or multi-junction device configuration.

We gratefully acknowledge Jürgen Hüpkes, Stephan Haas, Carolin Ulbrich, and Juraj Hotovy for constructive discussions. This work was carried out in the framework of the project "Nanospec", funded by the European Community's Seventh Framework Programme (FP7/2007-2013) under grant agreement no 246200.

References

1. E. Yablonovitch, G.D. Cody, IEEE Trans. Electron Devices **29**, 300 (1982)
2. H.W. Deckman et al., Appl. Phys. Lett. **42**, 968 (1983)
3. O. Kluth et al., Thin Solid Films **351**, 247 (1999)
4. M. Ermes et al., J. Appl. Phys. **113**, 073104 (2013)
5. J.I. Owen et al., Phys. Stat. Sol. A **208**, 109 (2011)
6. J. Bailat et al., in *Proceedings of the 25th European Photovoltaic Solar Energy Conf./5th World Conf. Photovoltaic Energy Convers, Valencia, 2010*, p. 2720
7. M. Python et al., Prog. Photovolt.: Res. Appl. **18**, 491 (2010)
8. S. Hänni et al., IEEE J. Photovolt. **99**, 1 (2012)
9. F. Ruske et al., J. Appl. Phys. **107**, 013708 (2010)
10. T. Minami et al., J. Vacuum Sci. Technol. A **17**, 1822 (1999)

11. R.G. Gordon, MRS Bulletin **25**, 52 (2000)
12. A. Lambertz et al., Sol. Energy Mater. Sol. Cells **119**, 134 (2013)
13. S. Kim et al., Sol. Energy Mater. Sol. Cells **119**, 26 (2013)
14. M. Boccard et al., IEEE J. Photovolt. **2**, 229 (2012)
15. M. Kambe et al., in *Proceedings of the 3rd World Conf. Photovoltaic Energy Conversion, Osaka, 2003*, Vol. 2, p. 1812
16. J. Krc et al., Thin Solid Films **518**, 3054 (2010)
17. K.C. Lai et al., Sol. Energy Mater. Sol. Cells **94**, 397 (2010)
18. C. Battaglia et al., Appl. Phys. Lett. **96**, 213504 (2010)
19. C. Battaglia et al., J. Appl. Phys. **109**, 114501 (2011)
20. T. Koida et al., Jpn J. Appl. Phys. **28**, L685 (2007)
21. M. Wimmer et al., Thin Solid Films **520**, 4203 (2012)
22. S. Neubert et al., Prog. Photovolt.: Res. Appl. **22**, 1285 (2014)
23. J. Geissbühler et al., IEEE J. Photovolt. **4**, 1055 (2014)
24. H. Sai et al., in *Proceeding of the MRS conference, San Francisco, 2013*, Vol. 1536, p. 3
25. E. Kobayashi et al., in *Proceedings of the 28th European Photovoltaic Solar Energy Conference and Exhibition, Paris, 2013*, p. 691
26. T.C.M. Müller et al., Energy Procedia **10**, 76 (2011)
27. J.C. Goldschmidt et al., in *Renewable Energy and the environment* (Optical Society of America, 2013), paper PT3C.2
28. J. Owen, Ph.D. thesis, RWTH Aachen University, 2011
29. B. Rech et al., Thin Solid Films **511**, 548 (2006)
30. B.E. Pieters et al., J. Appl. Phys. **105**, 044502 (2009)
31. B.E. Sernelius et al., Phys. Rev. B **37**, 10244 (1988)
32. E. Burstein, Phys. Rev. **93**, 632 (1954)
33. M. Berginski et al., Thin Solid Films **516**, 5836 (2008)
34. A. Pflug et al., Thin Solid Films **455**, 201 (2004)
35. S. Takata et al., Thin Solid Films **135**, 183 (1986)
36. T. Minami, H. Sato, K. Ohashi, T. Tomofuji, S. Takata, J. Cryst. Growth **117**, 370 (1992)
37. C. Ulbrich, Prog. Photovolt.: Res. Appl. **21**, 1672 (2013)
38. J. Escarre et al., Sol. Energy Mat. Sol. Cells **98**, 185 (2012)

Cite this article as: Etienne Moulin, Thomas Christian Mathias Müller, Marek Warzecha, Andre Hoffmann, Ulrich Wilhelm Paetzold, Urs Aeberhard, Highly transparent front electrodes with metal fingers for p-i-n thin-film silicon solar cells, EPJ Photovoltaics **6**, 60501 (2015).